Nanoscale

Accepted Manuscript

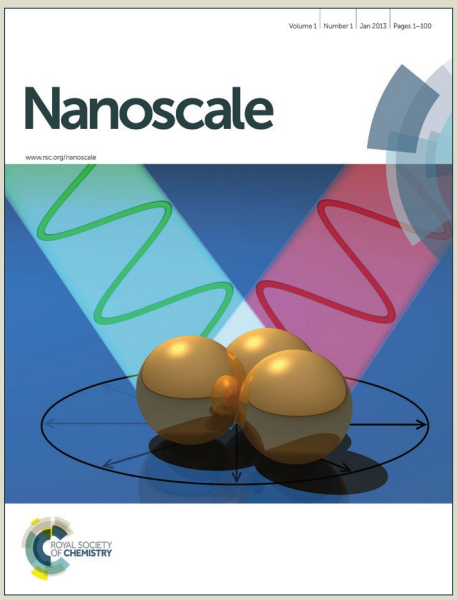

ROYAL SOCIETY OF CHEMISTRY

www.rsc.org/nanoscale

Journal Name

COMMUNICATION

Transparent Projection Screen Based on Plasmonic Ag Nanocubes

Koichiro Saito and Tetsu Tatsuma*

Received 00th January 20xx,
Accepted 00th January 20xx

DOI: 10.1039/x0xx00000x

www.rsc.org/

A transparent and colourless projection screen is fabricated by depositing a silver nanocube sub-monolayer on a titania thin film. Backward scattering of the silver nanocubes is enhanced by titania in the blue and red regions, in which human eyes are less sensitive. As a result, this screen, which is cost-effective even for large areas, allows projection of full colour images.

A transparent projection screen allows us to see images projected on it and a view behind it simultaneously. It can therefore be applied to, for instance, head-up displays, which show car navigation information on a car windshield, and shop windows that can show translucent images and movies. There are several different types of materials for transparent projection screens. In the case of microlens array-based screens, a complex microfabrication technique is required.[1,2] On the other hand, dispersing high refractive index particles such as nanodiamond into transparent matrix is a much more common and simple way to produce large screens.[3] Metal nanoparticles also scatter light strongly on the basis of localized surface plasmon resonance (LSPR).[4] In the case of plasmonic nanosphere, its absorption cross section is proportional to its volume[5] and scattering cross section is roughly proportional to the square of its volume.[6] However, since LSPR wavelength is redshifted as the particle volume increases, blue light is relatively difficult to scatter.[7] A plasmonic screen for scattering blue light has been developed by dispersing mid-size Ag nanospheres (~60 nm diameter) in a polymer matrix, whereas the transmitted light looks yellow due to relatively strong absorption of blue light by the mid-size nanospheres.[8] As the luminosity function shows (Fig. 1a), human eyes are not very good at detecting blue light. In addition, larger power is necessary to emit blue light. Development of screens efficiently scatter blue light is therefore important. Transparent projection screens for full colour images are, however, also required to scatter light in the other colours. In this research, we developed a plasmonic transparent screen for full-colour projection, which strongly scatter blue light in particular, by using a sub-monolayer of almost monodisperse Ag nanocubes. Although the screen strongly scatters blue light, its transmitted light is almost colourless.

We prepared the transparent screen by depositing Ag nanocubes onto a TiO_2 thin film. Ag nanocubes exhibit interesting properties including strong absorption, scattering and optical near field.[9-13] In addition, when a Ag nanocube is placed on a solid substrate, its LSPR mode splits into two modes, the distal and proximal modes.[14] Electron oscillation and accompanying electric field oscillation are localized at around the top of the nanocube for the distal mode and at the bottom for the proximal mode. The peak splits gradually as the refractive index of the substrate increases,[15] and splits almost completely on TiO_2, which has a high refractive index.[10,16,17] This allows strong scattering in the blue region (380-490 nm). The scattering and absorption spectra of a Ag nanocube essentially depend on the nanocube size and the TiO_2 thickness. Therefore, we first optimize these factors by a finite difference time-domain (FDTD) method, in terms of scattering properties, and then experimentally prepared the transparent projection screen.

Backward scattering spectra of Ag nanocubes with different sizes (edge length: 80, 100, and 120 nm) on sufficiently thick anatase TiO_2 (800 nm) under normally incident light are calculated by using Lumerical FDTD solutions, and the results are shown in Fig. 1a. The simulation domain (550 × 550 × 550 nm) consisted of 4 nm cubic cells and the central region (400 × 400 × 400 nm) was further meshed with a three-dimensional grid of 2 nm spacing. Backward scattering from the nanocube was monitored by a square screen set 20 nm apart from the TiO_2 surface. In the calculation model, the curvature radius of the Ag nanocube corner is 10 nm and the nanocubes are located 2 nm away from the TiO_2 considering the thickness of the protective reagent, poly(vinylpyrrolidone)

Institute of Industrial Science, The University of Tokyo, 4-6-1 Komaba, Meguro-ku, Tokyo 153-8505, Japan

Electronic Supplementary Information (ESI) available: Preparation of Ag nanocubes. Calculated values for a Ag nanocube on TiO_2 (Tables S1 and S2). See DOI: 10.1039/x0xx00000x

on the nanocube.[18] The dielectric functions for Ag,[19] anatase TiO_2,[20] and glass[19] used in the calculations are based on the literature data.

As Fig. 1a shows, both distal (412 → 455 nm) and proximal (565 → 729 nm) mode peaks are redshifted as the particle size increases (80 → 120 nm). We conclude that the Ag nanocube with 100 nm edge length is the most suitable for the projection screen, because it exhibits scattering peaks in 400-440 nm and 640-680 nm wavelength regions, in which the luminosity factor is low. As the nanocube size increases, the scattering intensity also increases, but the nanocubes become more difficult to synthesize. This is another reason to sel the 100 nm cubes. However, in comparison with the blue ligh scattering, green and red light scattering is too weak for fu colour projection. We therefore changed the TiO_2 thickness to control the scattering peak intensities taking advantage of th optical interference.

In the case of front incidence, the light reflected from th highly refractive TiO_2 film interferes with the incident light. Accordingly, the electric field intensity of the light depends o the distance from the film surface.[11] If the TiO_2 film is thick enough, we have only to consider the reflection from the TiO_2 surface, at which the nanocube is placed. In this case, the electric field intensity at the TiO_2 surface is the lowes because the phase of the reflected light is shifted from that o the incident light by π. Therefore, excitation of the proxima mode, which is responsible for the green and red scattering, i suppressed. On the other hand, the electric field intensit the highest at the location λ/4 away from the TiO_2 surface (λ = wavelength). The distal mode is thus excited strongly, w the edge length of a Ag nanocube is close to λ/4. It is therefore

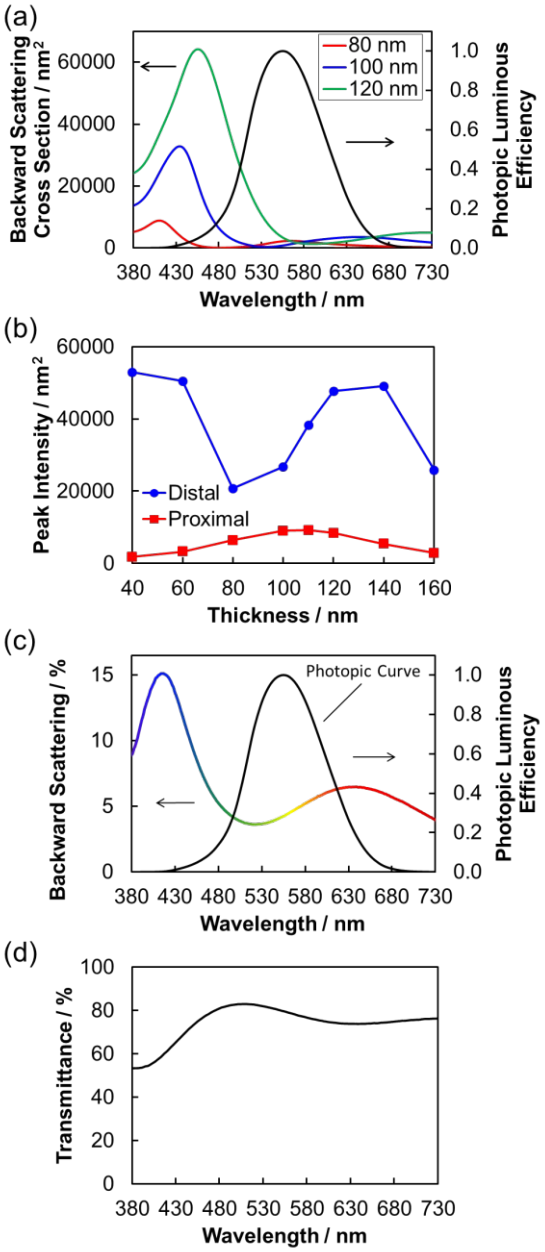

Fig. 1 (a) Backward scattering spectra simulated for Ag nanocubes deposited on thick TiO_2 (800 nm). (b) Relationships between the TiO_2 thickness and the distal and proximal mode backward scattering peak intensities of a 100 nm Ag nanocube on TiO_2. (c) Backward scattering spectrum and (d) transmission spectrum of the experimentally prepared sample with a Ag nanocube (~100 nm) submonolayer on a ~110 nm thick TiO_2. A photopic luminosity curve is also shown in (a) and (c).

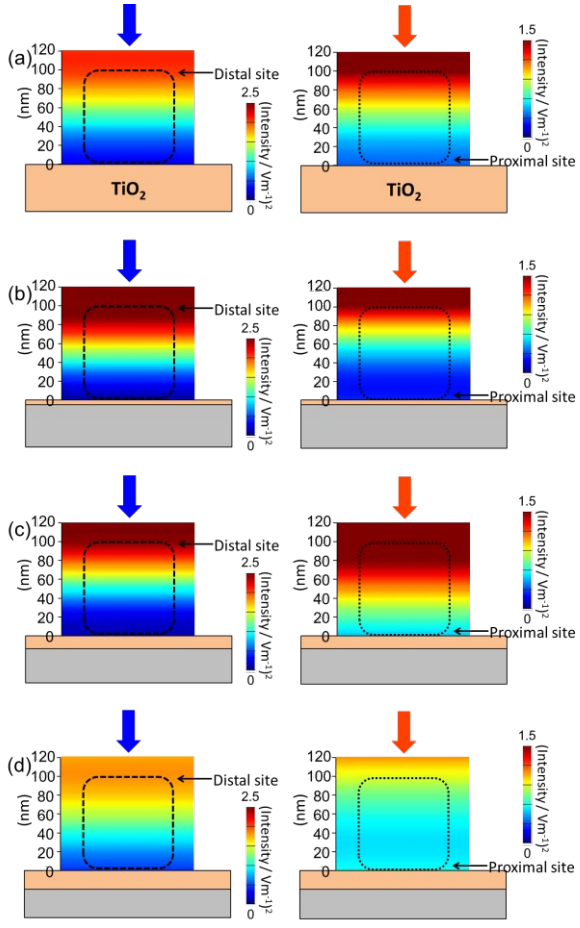

Fig. 2 Spatial distributions of electric field intensity in the vicinity of the surface of (a) a 800 nm thick TiO_2 slab, (b) 40, (c) 110, and (d) 160 nm thick TiO_2 films on a glass slab. Incident light wavelengths are (a) 437 and 648 nm, (b) 432 and 603 nm, (c) 432 and 636 nm, and (d) 449 and 700 nm for left and right figures, respectively.

reasonable that the blue light scattering due to the distal mode is much stronger than the green and red light scattering based on the proximal mode when the nanocube size is 100 nm and λ is about 400 nm. The spatial distributions of the square of the electric field intensity E^2, which is proportional to the photon density, at extinction (= absorption + scattering) peak wavelengths for the distal and proximal modes are shown in Fig. 2a. On the other hand, in the case of a TiO_2 thin film coated on a glass plate, light reflected from the TiO_2/glass interface and light reflected multiply in the TiO_2 film also take part in the interference. The ratio of the LSPR intensity between the distal mode and the proximal mode can therefore be controlled by changing the film thickness.

Fig. 2b-d show the spatial distributions of the electric field intensity in the case of 40, 110, and 160 nm thick TiO_2 film. Note that the optical thickness of 40 nm thick TiO_2 is 106 nm at λ = 430 nm, because the refractive index is 2.66 at this λ. Regarding the distal regions, in which distal mode oscillation occurs, the electric field intensity is high when the film is 40 or 110 nm thick, whereas the intensity is low for the 160 nm thick film. On the other hand, the electric field intensity at the proximal regions, in which proximal mode oscillation takes place, are high for the 110 or 160 nm thick film, whereas that for the 40 nm thick film is low. The difference in the electric field intensities is expected to correspond to that of the extinction cross section for each LSPR mode of the Ag nanocube on the TiO_2 film. Those values calculated for a 100 nm Ag nanocube are therefore listed in Table S1 (the distal region is 72-102 nm and the proximal region is 2-32 nm away from the TiO_2 surface). The values of the extinction cross sections and E^2 are normalized at the corresponding values for the 40 nm thick TiO_2 film. Each normalized extinction value is in broad agreement with that for the corresponding E^2 value, except for the proximal mode values for the 160 nm thick TiO_2 film. The electric filed intensity that Ag nanocube receives may be altered in some cases by the existence of the nanocube itself.

We investigated the scattering intensities of the Ag nanocube (100 nm) on the TiO_2 film with different thickness to seek out the thickness appropriate for transparent screens. The backward scattering intensities of the two modes are plotted against the TiO_2 thickness in Fig. 1b. The scattering intensity of the proximal mode is high when the TiO_2 thickness is 100-120 nm. Additionally, we calculated the viewing angle dependence of the backward scattering in the case of 110 nm thick TiO_2. The ratio of the scattering intensity at 455 nm (blue light) to that at 636 nm (red light) gradually decreased as the angle increases (Table S2). Therefore, a colour image projected on the screen may be viewed with a similar colour tone at a viewing angle less than 30°.

Therefore, we experimentally prepared ~110 nm thick TiO_2 film on one side of a borosilicate glass plate (Tempax®) by a sol-gel dip coating process (withdrawal rate was 3 mm s^{-1}, calcined at 500 °C for 1 h) from a titaniumalkoxide ethanol solution (NDH-510C, Nippon Soda). We synthesized Ag nanocubes with approximately 100 nm edge length by a polyol method[11,21] and deposited them on the TiO_2 film (coverage Γ ~ 3.5 × 10^8 particles cm^{-2}) by casting an ethanolic dispersion of the nanocubes followed by evaporation of ethanol and a rinse with deionized water. Fig. 1c shows the backward scattering spectrum of the fabricated sample measured by a spectrophotometer (V-670, Jasco) with an integrating sphere together with the photopic luminosity curve. The peak wavelength of the distal mode is 417 nm and that of the proximal mode is 638 nm; light is strongly scattered in the wavelength range where the luminosity factor is low. Since the nanocubes have a certain size dispersion, the experimentally obtained peaks are broader than the theoretically calculated peaks and light can be scattered in the whole visible range even in between the two peaks. On the other hand, the transmittance spectrum shown in Fig. 1d is almost flat, so that the transmitted light is expected to be virtually colourless.

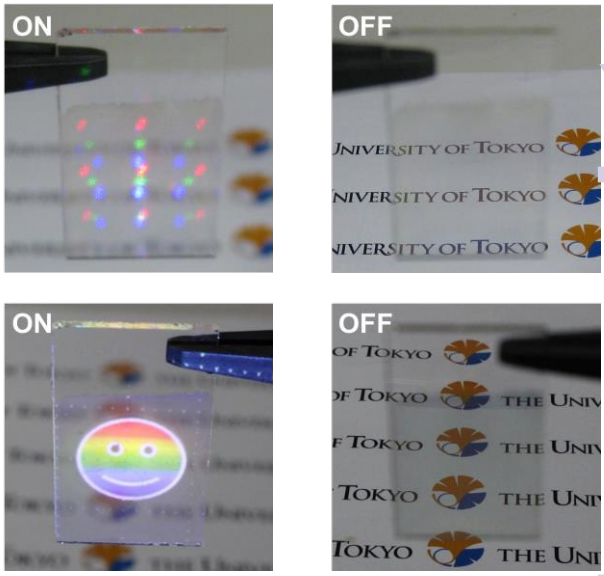

Fig. 3 Photographs of the plasmonic transparent projection screen. (a) (left) The screen is irradiated by blue, green, and red lasers. The number of the light spot is increased using a diffraction grating. (b) (left) A colour image is projected by use of an LCD projector. (a, b) (right) No image is projected.

Note that the scattering cross section for the calculated data can be converted into scattering intensity. For instance, in the case of the distal mode of a single 100 nm Ag nanocube shown in Fig. 1a, the scattering intensity at the peak wavelength is 11.6% if the particle density is the same as that for the experiment (Γ = 3.5 × 10^8 particles cm^{-2}). The calculated value could be lower than the experimentally observed value because backward scattering from the nanocube is monitored by a square screen with finite area (500 × 500 nm) set 250 nm apart from the air-TiO_2 interface.

We demonstrated projection of colour images on the film. Fig. 3 shows a photograph of the sample irradiated with blue, green, and red lasers (450, 532, and 635 nm, respectively, from laser diodes and a photograph of a colour image projected on the sample by use of an LCD projector (Epson EB-1761W, peak wavelengths for blue, green, and red light are 442, 552, and 612 nm, respectively). Full colour images can be displayed on the film, although it is colourless and transparent.

where no image is projected.

Although Ag nanoparticles on TiO_2 could be oxidized gradually[22] because of plasmon-induced charge separation,[23] it can be suppressed by isolating the particles from humid air.[24] For instance, we confirmed experimentally that the Ag nanocubes on TiO_2 can be protected by coating them with a ~20 nm thick poly(vinyl chloride) film, while the spectrum is almost retained (i.e. the shift of distal mode peak is ~30 nm).

In conclusion, here we developed a transparent and colourless projection screen by using a TiO_2 film and a plasmonic Ag nanocube sub-monolayer. This screen, which is cost-effective even for large areas, allows projection of full colour images.

Acknowledgements

This work was supported in part by a Grant-in-Aid for Scientific Research No. 25288063.

Notes and references

1 M. K. Hedili, M. O. Freeman and H. Urey, *Optics Express*, 2013, **21**, 24636.
2 K. Hong, J. Yeom, C. Jang, G. Li, J. Hong and B. Lee, *Optics Express*, 2014, **22**, 14363.
3 J. F. Goldenberg and T. S. McKechnie, *J. Opt. Soc. Am. A*, 1985, **2**, 2337.
4 H. A. Atwater and A. Polman, *Nat. Mater.*, 2010, **9**, 205.
5 S. Link and M. A. El-Sayed, *J. Phys. Chem. B*, 1999, **103**, 8410.
6 P. K. Jain, K. S. Lee, I. H. El-Sayed and M. A. El-Sayed, *J. Phys. Chem. B*, 2006, **110**, 7238.
7 T. Jensen, L. Kelly, A. Lazarides and G. C. Schatz, *J. Cluster Sci.*, 1999, **2**, 295.
8 C. W. Hsu, B. Zhen, W. Qiu, O. Shapira, B. G. DeLacy, J. D. Joannopoulos and M. Soljačić, *Nat. Commun.*, 2014, **5**, 3152.
9 A. Moreau, C. Ciracì, J. J. Mock, R. T. Hill, Q. Wang, B. J. Wiley, A. Chilkoti and D. R. Smith, *Nature*, 2012, **492**, 86.
10 A. Bottomley and A. Ianoul, *J. Phys. Chem. C*, 2014, **118**, 27509.
11 K. Saito and T. Tatsuma, *Adv. Opt. Mater.*, 2015, **3**(7), 8835.
12 K. Leonard, J. You, Y. Takahashi, H. Yonemura, J. Kurawaki and S. Yamada, *J. Phys. Chem. C*, 2015, **119**, 8829.
13 T. Kawawaki, H. Wang, T. Kubo, K. Saito, J. Nakazaki, H. Segawa and T. Tatsuma, *ACS Nano*, 2015, **9**, 4165.
14 L. J. Sherry, R. Jin, C. A. Mirkin, G. C. Schatz and R. P. Van Duyne, *Nano Lett.*, 2005, **5**, 2034.
15 S. Zhang, K. Bao, N. J. Halas, H. Xu and P. Nordlander, *Nano Lett.*, 2011, **11**, 1657.
16 I. Tanabe and T. Tatsuma, *Nano Lett.*, 2012, **12**, 5418.
17 I. Tanabe and T. Tatsuma, *Chem. Lett.*, 2014, **43**, 931.
18 E. Ringe, J. M. McMahon, K. Sohn, C. Cobley, Y. Xia, J. Huang, G. C. Schatz, L. D. Marks and R. P. Van Duyne, *J. Phys. Chem. C*, 2010, **114**, 12511.
19 D. W. Lynch and W. R. Hunter, In Handbook of Optical Constants of Solids; E. D. Palik, Ed.; Academic Press: New York, 1985.
20 G. E. Jellison, L. A. Boatner, J. D. Budai, B. S. Jeong and D. P. Norton, *J. Appl. Phys.*, 2003, **93**, 9537.
21 S. H. Im, Y. T. Lee, B. Wiley and Y. Xia, *Angew. Chem. Int. Ed.*, 2005, **44**, 2154.
22 Y. Ohko, T. Tatusma, T. Fujii, K. Naoi. C. Niwa, Y. Kubota and A. Fujishima, *Nature Mater.*, 2003, **2**, 29.
23 Y. Tian and T. Tatsuma, *J. Am. Chem. Soc.*, 2005, **127**, 7632.
24 K. Naoi, Y. Ohko and T. Tatsuma *Chem. Commun.*, 2005, 1288.